J Mol Model (2005) 11: 385–391
DOI 10.1007/s00894-005-0268-3

ORIGINAL PAPER

Slawomir Filipek

Organization of rhodopsin molecules in native membranes of rod cells–an old theoretical model compared to new experimental data

Received: 2 November 2004 / Accepted: 1 February 2005 / Published online: 1 June 2005

Abstract It has been shown that rhodopsin forms an oligomer in the shape of long double rows of monomers. Because of the importance of rhodopsin as a template for all G protein-coupled receptors, its dimeric, tetrameric and higher-oligomeric structures also provide a useful pattern for similar structures in GPCRs. New experimental data published recently are discussed in the context of a proposed model of the rhodopsin oligomer 1N3M deposited in the protein data bank. The new rhodopsin structure at 2.2 Å resolution with all residues resolved as well as an electron cryomicroscopy structure from 2D crystals of rhodopsin are in agreement with the 1N3M model. Accommodation of movement of transmembrane helix VI, regarded as a major event during the activation of rhodopsin, in a steady structure of the oligomer is also discussed.

Keywords GPCR · Rhodopsin · Membrane protein · Oligomerization

Abbreviations GPCR: G protein-coupled receptor · PDB: Protein data bank · TMH: Transmembrane helix · ROS: Rod outer segment · ET: Evolutionary trace

Introduction

G protein-coupled receptors (GPCRs) represent a very large superfamily of receptors essential for signaling across plasma membranes [1–3]. In humans, about 1,000 genes encode GPCRs, half of them odor and taste receptors and the other half receptors of endogenous ligands and light [4, 5]. Each GPCR responds to a single or a few ligands by activating G proteins. Then the trimeric $G_{\alpha\beta\gamma}$ protein dissociates into G_{α} and $G_{\beta\gamma}$ and one of them (depending on the specific pathway) modulates enzymes and channels, giving rise to a highly amplified signaling cascade. Such processes are responsible for vision, taste, smell, neurotransmission and also involve responses to peptides, hormones, proteases, chemokines and others. Thus, GPCRs are important targets for pharmacological intervention [6] and a large fraction of current drugs is directed toward them [2]. Even though GPCRs are so ubiquitous, only a small fraction of their pharmacological potential is currently recognized [7].

Despite the broad range of possible actions of GPCRs, they all share a common seven α-helical transmembrane bundle structural design. The ligand-binding site is located either at the extracellular region or within the transmembrane α-helical bundle, and the cytoplasmic loops are responsible for coupling to G proteins and other effector proteins. The most extensively studied GPCR is rhodopsin. It is expressed in rod photoreceptor cells involved in scotopic vision. Rhodopsin resides in the intracellular membranes that form stacks of flattened discs in the rod outer segment (ROS), the long subcellular compartment dedicated to phototransduction. Rhodopsin is the only GPCR with a 3D structure resolved at atomic detail [8]. The rhodopsin structure may serve as a template for building other GPCRs, since the transmembrane segments of these receptors are highly homologous [9]. Other components of the signaling machinery have conserved structures as well. The high-resolution structures of G proteins as well as arrestins, proteins that deactivate GPCRs, show only small structural variance [10]. In addition, the mechanism of receptor activation appears to be conserved for all members of the GPCR superfamily [11, 12]. These findings suggest that rhodopsin is not only a structural template but is also mechanistically analogous to other GPCRs.

S. Filipek
International Institute of Molecular and Cell Biology,
4 Ks. Trojdena St, 02-109 Warsaw, Poland
E-mail: sfilipek@iimcb.gov.pl
Tel.: +48-22-5970722
Fax: +48-22-5970715

The recently demonstrated oligomerization of rhodopsin [13] is also an important feature of other GPCRs and also affects their function. The classical idea is that GPCRs function as monomeric proteins. However, a growing body of pharmacological, biochemical and biophysical data suggests that these receptors form functional homo- and heterodimers as well as higher oligomers see [14] and references therein. Furthermore, their oligomeric assemblies have important functional roles [15]. Several studies have shown that G-protein coupling, downstream signaling and regulatory processes such as internalization are influenced by the dimeric nature of the receptors. The concept of dimerization is also important in the development and screening of drugs. In particular, the changes in ligand-binding and signaling properties that accompany and influence homo- and heterodimerization could give rise to new classes of pharmacologically active compounds.

Materials and methods

Our current model of the rhodopsin dimer [16, 17] is based directly on the 1N3M model of the rhodopsin oligomer [13] deposited in the protein data bank (PDB). The basis for this model was the crystal structure of rhodopsin [18] (PDB access code 1HZX). Based on atomic force microscope (AFM) measurements of distances between rhodopsins in the paracrystals as well as energetic considerations, a model was constructed with helices IV and V forming an interface between rhodopsin molecules. Oligomers in the model are built from separate dimers and linked together by a long cytoplasmic loop between helices V and VI. A dimer is a repetitive motif in the oligomer (forming a double row of monomers). Therefore tetramers and higher structures are connected in an identical manner. Structure optimization and molecular dynamics were carried out using the CVFF force field in the discover program (InsightII 2000, Accelrys Inc.). Atomic charges were determined by minimizing the electrostatic energy of the system while varying the charges. A series of short molecular dynamics simulations, up to 100 ps in a single run, was used to build a reliable system of interacting proteins. After each molecular dynamics run, optimization of the whole structure was performed (maintaining frozen parts when necessary).

The 1N3M model was improved by the addition of phospholipids. Specifically, three types of phospholipids were used with phosphatidylcholine headgroups on the intradiscal side and phosphatidylethanolamine and phosphatidylserine headgroups (three times more phosphatidylethanolamine headgroups than phosphatidylserine) on the cytoplasmic side to mimic native membranes of ROS [19, 20]. All three types of phospholipids contain the saturated stearoyl chain (18 : 0) in the *sn*1 position and the polyunsaturated docosahexaenoyl chain (22 : 6n-3) in the *sn*2 position. Phospholipids were inserted between rhodopsin monomers and the complex was optimized by molecular dynamics followed by energy minimization with the rhodopsin monomers frozen in their initial positions. Next, the complex was subjected to several steps of short molecular dynamics simulations followed by energy minimization to remove disallowed contacts. The distances between the rhodopsin monomers in the paracrystal remained unchanged after addition of the phospholipids and optimization of the model without any constraints. A longer molecular dynamics run, up to 500 ps in a periodic box using the NAMD2 software [21] with the CHARMM27 force field was used to validate that the oligomer model is stable.

Results

AFM measurements revealed the oligomeric structure of rhodopsin in native rod cell disc membranes [13]. This structure of rhodopsin oligomer is composed of double rows of monomeric units. Following this scheme and geometric constraints obtained from a paracrystal (distance between rhodopsins 3.8 nm, repetitive unit of double rows 8.4 nm and an angle between lattice vectors 85°), a model was assembled (1N3M access code in PDB) as noted in "Materials and methods". Other corrections, mainly the addition of phospholipids did not change the structure and distances of the oligomer. The main unit in the model is a non-covalent dimer formed by interacting transmembrane helices IV and V. The double row is assembled of such dimers and forms a second lattice vector nearly perpendicular (85°) to the line connecting monomers in a dimer (Fig. 1a). Adjacent rows of dimers are in contact with each other with transmembrane helix I forming an interface. It is characteristic of this model that an interface between adjacent dimers is formed by a long cytoplasmic loop between TMH-V and TMH-VI. This loop connects nearby amino acids of TMH-I and TMH-II from the preceding and subsequent dimers in a row. Because of the vital role of this loop and the fact that some amino acids from this fragment were absent in previous structures of rhodopsin, it is important to compare the model with new experimental data.

Figure 1b shows the cytoplasmic view of the oligomeric structure 1N3M of rhodopsin surrounded by phospholipids. The row of rhodopsin dimers runs vertically together with adjacent rows. Rhodopsin molecules in a dimer are in tight contact involving TMH-IV and TMH-V, while rhodopsins from different rows of dimers contact via TMH-I. The loop between helices TMH-V and TMH-VI (C-III) glues separate dimers together. Phospholipids flow on the left and right side of the central double row and these channels are two phospholipids wide. There are also thinner channels one phospholipid wide perpendicular to the wider ones and hidden below extended cytoplasmic loops C-III of the rhodopsin molecules.

The recently published structure of rhodopsin pushes the resolution limit to 2.2 Å . The new structure completely resolves the polypeptide chain and provides further details of the chromophore binding site (PBD access code 1U19) [22]. Because the space group ($P4_1$) was the same as in the earlier structures of rhodopsin, the previous trace of the backbone, even around the missing parts, is retained. The other data from Schertler's group (PBD accession code 1GZM) [23] come from a crystal belonging to another crystallographic group ($P3_1$). These data, resolved to 2.65 Å, show a different orientation of the cytoplasmic loop between TMH-V and TMH-VI, whereas the C-terminal region is not seen at all, in contrast to the structure from $P4_1$ space group crystals (Table 1). Both crystal structures represent dimers of rhodopsin. Unfortunately, this is not a native dimer since the monomers adopt a bottom-up position to each other. An interface is formed by TMH-I in 1U19 and TMH-V in 1GZM. Such bottom-up arrangements are more stable in the absence of a membrane, which highlights the great role of phospholipids in forming the proper interface in a native rhodopsin dimer. A comparison of the 1U19 and 1GZM structures is shown on Fig. 2, whereas all three structures, with emphasize on the dimeric interfacial loop, are shown on Fig. 3.

The structures 1U19 and 1GZM are nearly identical in their extracellular and membrane parts. The differences are confined to cytoplasmic loops and C-termini. Whereas 1U19 is completely resolved, 1GZM lacks amino acids 327–329 and 333–348, all in the C-terminus. Nevertheless, not only the C-terminus is different. The cytoplasmic loop between TMH-III and TMH-IV (C-II) is slightly moved but the main difference is in the cytoplasmic loop between TMH-V and TMH-VI (C-III). In 1U19, this loop folds outside the rhodopsin, presumably along the membrane surface, while in 1GZM it is in a vertical position (Fig. 2 and magnification in Fig. 3). A part of this loop is in contact with the same part in the adjacent symmetrical molecule in 1U19, while the same loop in the 1GZM structure has no contact with other

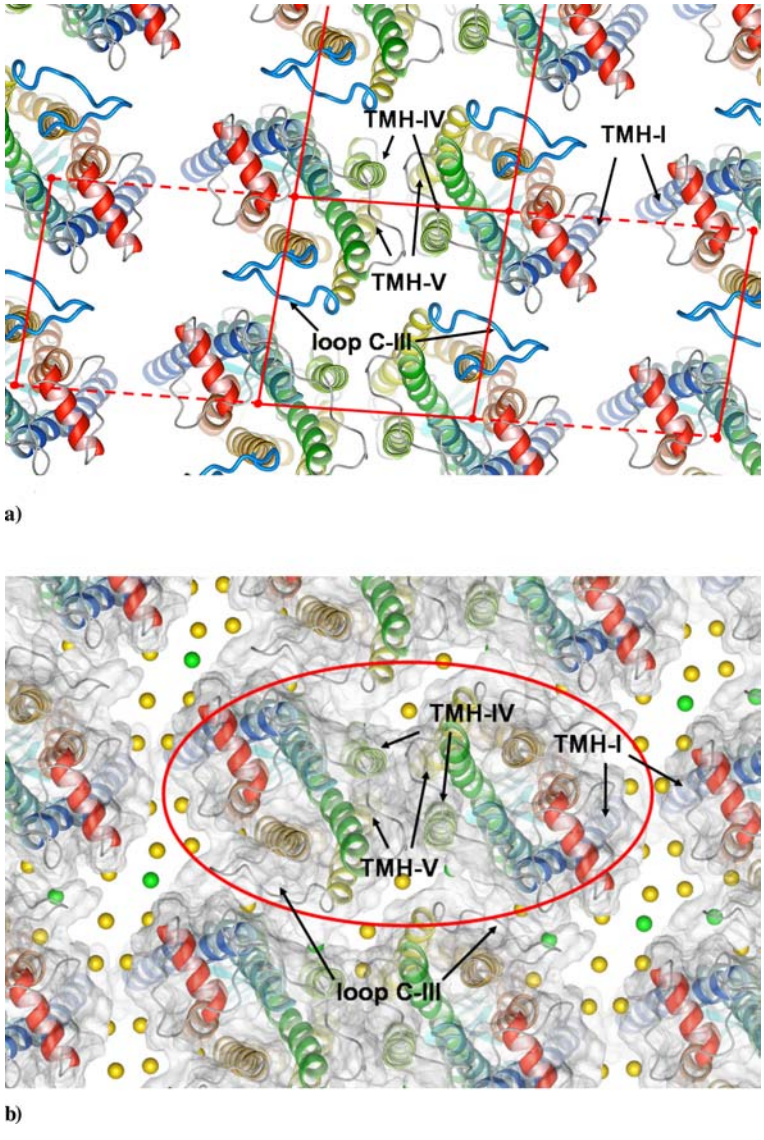

Fig. 1 The structure of rhodopsin oligomer model 1N3M in the membrane. View from cytoplasmic side. **a** Organization of the oligomer. AFM constraints shown as a *red net*. The loop C-III emphasized by *blue color* and thickening. **b** The same view with transparent surfaces of the rhodopsin molecules. Structure of a single dimer marked by ellipse. Positions of phospholipids are denoted by *dark yellow* (ethanolamine heads) and *green* (serine heads) spheres

Table 1 Comparison of data of crystal structures of rhodopsin 1HZX, 1U19 and 1GZM. The theoretical model of the oligomeric state of rhodopsin 1N3M was created based on the 1HZX structure

PDB accession code	1HZX (1N3M)	1U19	1GZM
References	[18, 13]	[22]	[23]
Space group	$P4_1$	$P4_1$	$P3_1$
Resolution (Å)	2.80	2.20	2.65
Asymmetric unit	Bottom-up dimer	Bottom-up dimer	Bottom-up dimer
Contact TMH in dimer	I–I	I–I	V–V
Lacking amino acids	236–240 (C-III loop), 331–333 (C-term.)	None	327–329 (C-term.), 333–348 (C-term.)

rhodopsin molecules in the crystal. This means that the loop is highly movable and changes its shape easily, so it could bind to another rhodopsin regardless of possible deformations of the loop. The modeled loop in 1N3M is similar to that in 1U19 (Fig. 3) but more extended. The adjacent rhodopsin molecule in a modeled native dimer is farther away than in the crystal bottom-up dimer, so the loop C-III changes its shape to bind amino acids from TMH-I and TMH-II of the adjacent rhodopsin dimer.

The mobility of this loop can be seen on Fig. 4a, b. Two cytoplasmic loops C-II and C-III as well as the C-terminus are associated with very high thermal factors. The values for the loop C-III are below 110 in the 1U19 structure and up to 175 in the 1GZM structure, respectively. The loop in the latter structure is not bound to any other rhodopsin in the crystal, whereas in the former it binds to an adjacent symmetrical rhodopsin molecule, which significantly lowers its thermal movement. The C-terminus in the 1U19 structure is well resolved but is not seen in the 1GZM structure, possibly for the same reason. The conformation of this loop in the oligomer model differs from that in the 1U19 structure but is also extended and ready to bind another dimer. The loop in 1U19 cannot extend more because of the proximity of an adjacent rhodopsin in a crystal.

The structural information for rhodopsin and possibly the other GPCRs can not only be drawn from 3D crystals but also, however with lower resolution, from 2D crystals. Schertler's group reported a three-dimensional density map of bovine rhodopsin determined by electron cryomicroscopy of 2D crystals with $p22_12_1$ symmetry [24]. The final resolution was 5.5 Å in the membrane plane and about 13 Å perpendicular to it. It was enough to identify all seven transmembrane helices and their arrangement in the bundle. The structure found was in agreement with the arrangement known from the crystal structure. The unit cell contains four molecules; two dimers with upside-down monomers in tight contact with helices TMH-IV and TMH-VI. The distance between monomers is about 3.2 nm. However, monomers on the diagonal are in a top to top position and contact each other with TMH-I. The distance between them is about 4.4 nm. This number is close to that found in the 1N3M model for the corresponding distance between adjacent rhodopsins from separate double rows (8.4 − 3.8 nm = 4.6 nm). The mutual positions of monomers are different in 1N3M and in the structure

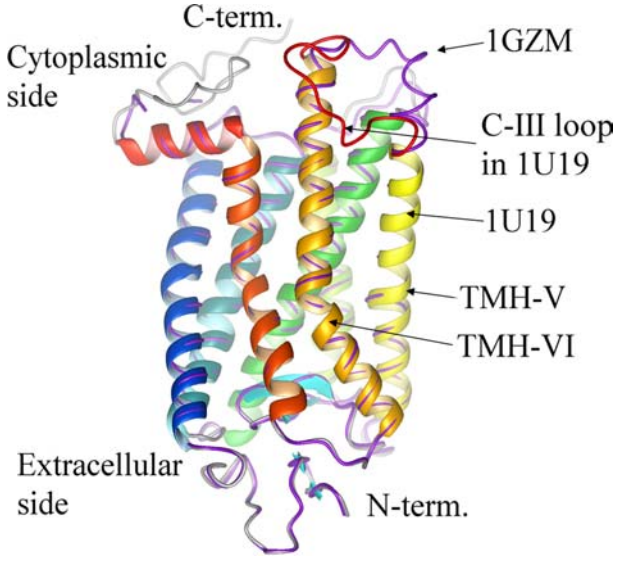

Fig. 2 Superimposition of the 1U19 rhodopsin structure (shown in secondary structure representation–colors of helices from *blue* TMH-I to *red* TMH-VII) and the 1GZM rhodopsin structure shown as *purple wire*. The loop between TMH-V and TMH-VI of 1U19 is *colored red* for better visibility

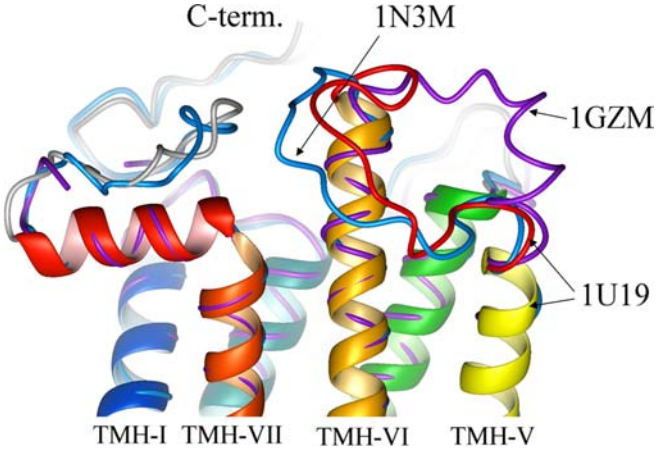

Fig. 3 Superimposition of the 1U19 rhodopsin structure (secondary structure representation–colors of helices from blue TMH-I to *red* TMH-VII), 1GZM rhodopsin structure (*purple wire*) and of a single monomer from the 1N3M rhodopsin oligomer model (*blue wire*). The loop between TMH-V and TMH-VI of 1U19 is colored *red* for better visibility

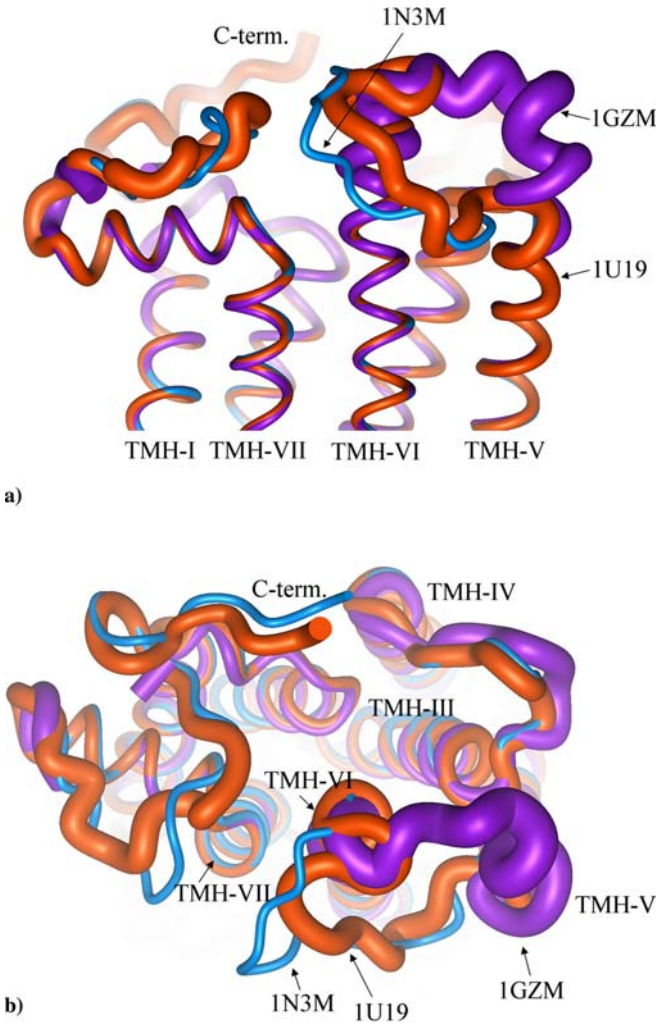

Fig. 4 Superimposition of the 1U19 (*red wire*), 1GZM (*purple wire*) and 1N3M (*blue wire*) rhodopsin structures. Size of the wires is proportional to thermal factors of backbone C_α atoms. **a** View parallel to the membrane; **b** view from the cytoplasmic side

derived from 2D crystals because of a different tilt of particular rhodopsin molecules.

Discussion

In recent years oligomerization of GPCRs has become evident experimentally. Biophysical methods based on luminescence and fluorescence-energy transfer have confirmed the existence of dimeric and even higher-oligomeric structures. It is suggested that dimerization plays a role in various aspects of receptor biogenesis and function. In some cases, receptors dimerize spontaneously and in others dimerization is promoted by a ligand. Rhodopsin, being the only GPCR with a resolved 3D structure, is still used as a template for structure building of other GPCRs. Currently, only the ground-state structure of rhodopsin has been described. Hence there modeling has an important role in elucidating the structural aspects of activation and signal passing, while taking the oligomeric state of rhodopsin into account.

Several methods have been used to predict the interfaces between proteins. Many of the computational methods used for modelling protein–protein complexes are similar to those used to model protein–ligand complexes. For instance, the DOCK program, was used in References [25, 26]. Because of the size of the computational task involved in docking two large protein structures, an approximation is often used to treat them as rigid bodies. The program FTDOCK was used in reference [27] to search for optimum interactions between two rigid proteins. This program was tested on various systems, including enzyme-inhibitor and antibody–antigen complexes. Adding an electrostatic component greatly improved the ability to find final solutions. Furthermore, side chain flexibility and the effect of solvation [28] were also implemented for this task. Protein–protein interfaces can also be modeled by molecular-surface fitting with surface flexibility implicitly addressed through liberal intermolecular penetration [29]. A fuzzy logic algorithm was also implemented for the shape-complementarity problem of interacting proteins [30, 31].

The above methods have been developed based on observations of complexes formed by globular and soluble proteins. Therefore, it is not known whether interfaces of membrane proteins, especially GPCRs, have similar features. For the small number of structural data of membrane proteins, and especially protein–protein complexes, it is difficult to apply the same techniques or to use the same scoring function. Among new methods, evolutionary trace (ET) [32] shows a high sensitivity for predicting the interfaces of protein complexes. Recently, this method was used for GPCRs [33] and it was reported that the evolutionary-trace residue cluster corresponds to the dimer interface. Dean et al. [34] also used the ET method for class A, B and C GPCRs and identified clusters of trace residues. However, the results of the experimental studies do not always agree with the predictions of the ET approach. Nemoto and Toh [35] improved the ET method by introducing structural information. The procedure involved projection of 3D coordinates onto a 2D plane, identification of exposed and inner residues, and identification of candidates for interface residues.

The method revealed the interface between rhodopsin molecules consisting of transmembrane helices IV and V, exactly as in the 1N3M model, with residues H152, M155, V162, W175 and E201 forming the interface. The authors applied this method to three other families of class A GPCRs, the dopamine receptors, the adrenergic receptors, and the muscarinic acetylcholine receptors, since the dimerization (or oligomerization) residues have been suggested for them from experiments, D_2R, [36, 37] β_2AR [38] and M_3R [39]. The positions of the predicted residues that form an interface in the D_2R dimer cor-

responded to TMH-IV, in agreement with experiment. The interfacial residues of β_2AR were all located on TMH-VI. For M_3R, transmembrane helices IV and V were found to be responsible for dimer formation. Furthermore, using this method it was possible to identify a second interface of rhodopsin. Predicted interface residues mapped on the oligomeric structure 1N3M were located on the interface between a pair of dimers, on TMH-V and TMH-VI. All loops were excluded from the ET analysis, so it is not confirmed whether the loop C-III (between TMH-V and TMH-VI) is involved in dimer–dimer interface formation. However, this is the longest loop at the cytoplasmic side and connects helices that contain the predicted residues so probably its role in inter-dimer interface formation is substantial.

The new rhodopsin structure 1U19 [22] with completely resolved polypeptide chain is also in agreement with the model of the rhodopsin oligomer 1N3M. The only difference is the loop C-III. In the oligomer model [13] this loop is more extended to bind the adjacent dimer in a row of dimers better. The other structure, 1GZM [23] derived from crystals in another space group, shows a different orientation of this loop. Because there is no contact with this loop in the crystal, the structure of the loop is regular with no lateral extensions. By contrast, the loop in 1U19 folds outside the rhodopsin because this loop is involved in a contact in the crystal. The same situation is found in the rhodopsin oligomer model but because the adjacent binding partner is farther away than in the 1U19 crystal, the loop is more extended. This loop covers the cytoplasmic layer of phospholipids, so only a few of them are visible (Fig. 1b). However, there is a space under the loop that phospholipids could fill and interact with rhodopsin. The extracellular part of rhodopsin is more compact, so that rhodopsin dimers do not interact there with each other and the only contact between them exists via the cytoplasmic loop C-III.

The recently obtained rhodopsin structure derived from 2D crystals determined by electron cryomicroscopy [24] demonstrates the existence of bottom-up dimers (not native) but also the contact of top to top monomers via TMH-I. Such a contact was also predicted by the oligomer model 1N3M, however, with a slightly longer distance and with different tilt. The driving force of formation of dimers in crystals is hiding (former) membrane hydrophobic surfaces. Formation of top to bottom dimers is preferred because of hiding more surface, so contact of the top to top type (via TMH-I), hiding less surface, is less significant in a crystal and the final structure is strongly influenced by more strongly bound neighbors.

The same research group determined the structure of rhodopsin photointermediate meta I in 2D crystals [40, 41]. The 5.5 Å resolution obtained is the same as in the dark rhodopsin structure, whereas the cell dimensions are about 3% smaller. Comparison of density maps with X-ray structures of the ground state of rhodopsin revealed that formation of Meta I does not involve large rigid-body movements of helices. The only rearrangement is located close to the kink of helix 6, at the level of the retinal chromophore. The Meta I state is achieved microseconds after bleaching so possibly this small amount of time is not enough for large movements of helices. The fully activated rhodopsin in the Meta II state is formed after milliseconds, so only this time is sufficient for larger structural changes. However, formation of Meta II is inhibited in 2D crystals. Activation of rhodopsin is accompanied by several structural movements and the biggest event is rotation and moving apart of TMH-VI. Unfortunately, this helix is involved in the formation of a contact with TMH-IV from an adjacent molecule in the crystal. In addition, the formation of Meta II in membranes depends on the lipid environment, with the Meta I–Meta II equilibrium shifting towards the Meta I state when the membrane contains increasing amounts of lipids with saturated fatty acyl chains. Thus, highly unsaturated lipids present in native membranes of ROS are essential for the formation of Meta II.

It is suggested that during activation of the rhodopsin, a cytoplasmic part of TMH-VI is rotated and moves away from the centre of the rhodopsin molecule [42, 43]. Such a movement is possibly a most spatial event during formation of Meta II. For a single rhodopsin, TMH-VI movement is accompanied by similar movement of the C-III loop. However, for the 1N3M oligomer model, this loop is involved in the inter–dimer interface and cannot be displaced (Fig. 1a, b). Fortunately the C-III loop is spread over the cytoplasmic part of the phospholipids even more, as is revealed by the 1U19 structure. Thus, adaptation of the C-III loop to the movement of TMH-VI is possible and the resulting rhodopsin structure is not strained (results not shown).

The oligomeric state influences the binding of other proteins to the cytoplasmic part of rhodopsin. Taking into account experimental difficulties, modelling can reveal to some extent aspects of rhodopsin activation, G protein binding, phosphorylation by rhodopsin kinase and deactivation by arrestin. Recently, the structure of the whole complex of trimeric G protein with a tetramer of rhodopsin was modelled [44] using 1N3M as a template. Simulations revealed that transducin (rhodopsin G protein) binds to the dimeric form of rhodopsin, whereas the adjacent dimer provides an additional surface to stabilize the complex. After dissociation the transducin beta–gamma subunit, the remaining alpha part can bind to a second transducin molecule and facilitate its docking to rhodopsin. Verification of such a model and its further fine tuning await results from experimental approaches.

Acknowledgements This study was supported by funds from Polish State Committee for Scientific Research grant 3P05F02625. Calculations were performed partly in ICM Computer Centre in Warsaw.

References

1. Mirzadegan T, Benko G, Filipek S, Palczewski K (2003) Biochemistry 42:2759–2767
2. Ballesteros J, Palczewski K (2001) Curr Opin Drug Discov Dev 4:561–574
3. Bartfai T, Benovic JL, Bockaert J, Bond RA, Bouvier M, Christopoulos A, Civelli O, Devi LA, George SR, Inui A, Kobilka B, Leurs R, Neubig R, Pin JP, Quirion R, Roques BP, Sakmar TP, Seifert R, Stenkamp RE, Strange PG (2004) Nat Rev Drug Discov 3:574–626
4. Nestler EJ, Landsman D (2001) Nature 409:834–835
5. Takeda S, Kadowaki S, Haga T, Takaesu H, Mitaku S (2002) FEBS Lett 520:97–101
6. Sautel M, Milligan G (2000) Curr Med Chem 7:889–896
7. Flower DR (1999) Biochim Biophys Acta Rev Biomembr 1422:207–234
8. Palczewski K, Kumasaka T, Hori T, Behnke CA, Motoshima H, Fox BA, Le Trong I, Teller DC, Okada T, Stenkamp RE, Yamamoto M, Miyano M (2000) Science 289:739–745
9. Filipek S, Teller DC, Palczewski K, Stenkamp R (2003) Annu Rev Biophys Biomol Struct 32:375–397
10. Ridge KD, Abdulaev NG, Sousa M, Palczewski K (2003) Trends Biochem Sci 28:479–487
11. Teller DC, Stenkamp RE, Palczewski K (2003) FEBS Lett 555:151–159
12. Ballesteros JA, Shi L, Javitch JA (2001) Mol Pharmacol 60:1–19
13. Fotiadis D, Liang Y, Filipek S, Saperstein DA, Engel A, Palczewski K (2003) Nature 421:127–128
14. Angers S, Salahpour A, Bouvier M (2002) Annu Rev Pharmacol Toxicol 42:409–435
15. Terrillon S, Bouvier M (2004) EMBO Rep 5:30–34
16. Liang Y, Fotiadis D, Filipek S, Saperstein DA, Palczewski K, Engel A (2003) J Biol Chem 278:21655–21662
17. Fotiadis D, Liang Y, Filipek S, Saperstein DA, Engel A, Palczewski K (2004) FEBS Lett 564:281–288
18. Teller DC, Okada T, Behnke CA, Palczewski K, Stenkamp RE (2001) Biochemistry 40:7761–7772
19. Giusto NM, Pasquare SJ, Salvador GA, Castagnet PI, Roque ME, Ilincheta de Boschero MG (2000) Prog Lipid Res 39:315–391
20. Saiz L, Klein ML (2001) Biophys J 81:204–216
21. Kale L, Skeel R, Bhandarkar M, Brunner R, Gursoy A, Krawetz N, Phillips J, Shinozaki A, Varadarajan K, Schulten K (1999) J Comput Phys 151:283–312
22. Okada T, Sugihara M, Bondar AN, Elstner M, Entel P, Buss V (2004) J Mol Biol 342:571–583
23. Li J, Edwards PC, Burghammer M, Villa C, Schertler GF (2004) J Mol Biol 343:1409–1438
24. Krebs A, Edwards PC, Villa C, Li JD, Schertler GFX (2003) J Biol Chem 278:50217–50225
25. Brooijmans N, Sharp KA, Kuntz ID (2002) Proteins 48:645–653
26. Shoichet BK, Kuntz ID (1996) Chem Biol 3:151–156
27. Gabb HA, Jackson RM, Sternberg MJE (1997) J Mol Biol 272:106–120
28. Jackson RM, Gabb HA, Sternberg MJE (1998) J Mol Biol 276:265–285
29. Duhovny D, Nussinov R, Wolfson HJ (2002) Algorithms Bioinformatics Proc 2452:185–200
30. Exner TE, Keil M, Brickmann J (2002) J Comput Chem 23:1176–1187
31. Exner TE, Keil M, Brickmann J (2002) J Comput Chem 23:1188–1197
32. Lichtarge O, Bourne HR, Cohen FE (1996) J Mol Biol 257:342–358
33. Madabushi S, Gross AK, Philippi A, Meng EC, Wensel TG, Lichtarge O (2004) J Biol Chem 279:8126–8132
34. Dean MK, Higgs C, Smith RE, Bywater RP, Snell CR, Scott PD, Upton GJG, Howe TJ, Reynolds CA (2001) J Med Chem 44:4595–4614
35. Nemoto W, Toh H (2005) Proteins 58:644–660
36. Guo W, Shi L, Javitch JA (2003) J Biol Chem 278:4385–4388
37. Lee SP, O'Dowd BF, Rajaram RD, Nguyen T, George SR (2003) Biochemistry 42:11023–11031
38. Hebert TE, Moffett S, Morello JP, Loisel TP, Bichet DG, Barret C, Bouvier M (1996) J Biol Chem 271:16384–16392
39. Zeng FY, Wess J (1999) J Biol Chem 274:19487–19497
40. Vogel R, Ruprecht J, Villa C, Mielke T, Schertler GFX, Siebert F (2004) J Mol Biol 338:597–609
41. Ruprecht JJ, Mielke T, Vogel R, Villa C, Schertler GF (2004) EMBO J 23:3609–3620
42. Altenbach C, Klein-Seetharaman J, Cai KW, Khorana HG, Hubbell WL (2001) Biochemistry 40:15493–15500
43. Hubbell WL, Altenbach C, Hubbell CM, Khorana HG (2003) Adv Prot Chem 63:243–290
44. Filipek S, Krzysko KA, Fotiadis D, Liang Y, Saperstein DA, Engel A, Palczewski K (2004) Photochem Photobiol Sci 3:628–638